Porous Supramolecularly Templated Optical Resonators Built in 1D Photonic Crystals

*Nuria Hidalgo, Mauricio E. Calvo, Martín G. Bellino, Galo J. A. A. Soler-Illia, and Hernán Míguez**

A synthetic route to attain photonic multilayers that presents controlled porosity only at the middle-layer level is shown. The spectral resonance associated with this porous layer shows strong sensitivity to the presence of vapors adsorbed or condensed within the void network, providing a potentially relevant material for gas detection. The importance of the interplay between pore and probe-molecule diameters is studied and its implications in size-selective detection are discussed.

1. Introduction

There is a growing interest in developing preparation procedures for multilayered materials that combine accessible porosity and high optical quality of structural origin. Potentially relevant applications of porous one-dimensional photonic crystals (1DPCs), which are defined as structures in which the refractive index varies periodically along one direction, have been identified in various fields such as sensing,[1–5] photovoltaics,[6] and lasing.[7] In all cases, new features or improved performance of the device are achieved as a result of the added functionality porosity brings. A multilayer structure of particular interest is that in which the refractive-index periodicity is broken by the presence of a middle layer of different thickness or refractive index, which acts as a controlled optical defect. By doing so, it is possible to create narrow transmission windows within the forbidden frequency gap at specific spectral regions. For such frequency ranges, an increase in the local density of states is also expected, which yields control over the luminescent properties of active species when embedded in the middle layer.[8] Due to the presence of this type of photonic mode, such structures are known as optical resonators. These structures have been thoroughly studied using layers of dense semiconducting materials as building blocks. Optical cavities have also been made of porous silicon layers prepared by electrochemically modulated anodic oxidation of silicon wafers, followed by acid etching. Such materials present well-defined dips in reflectance within high-reflectance spectral regions, typically in the visible or near-infrared regions, and an accessible void network that can be easily functionalized and infiltrated from both the gas and the liquid phase. The possibility to induce changes in the reflectance dip associated with the resonant mode through modifications in the environment has boosted the applications of these materials in chemical and biological sensing.[9] Also, TiO_2 multilayered resonators with modulated porosity have been achieved by glancing-angle physical-vapor deposition and their capability to respond optically to humidity changes in their direct environment has been demonstrated.[10]

Our group recently pioneered the use of metal oxides in the shape of both nanoparticles and mesostructured films for the construction of 1DPCs and of porous optical resonators within them.[11–14] In these resonators it has been possible to measure the first precise optical adsorption isotherms by taking advantage of the spectral shift of the narrow transmission window associated with the presence of the optical cavity that occurs when the partial pressure of the surrounding vapors is gradually increased.[2,15] These studies proved the complexity of the adsorption processes that take place in a multilayer in which films with different pore size alternate. Condensation within the larger pores is mediated by similar phenomena occurring in the smaller ones, hence analysis of the physicochemical mechanisms behind the changes observed in the optical-response results is complicated. These results were later confirmed by other groups in 1DPCs based on other types of porous layers.[16] In an alternative approach to the construction of environmentally responsive optical materials, dense 1DPCs have been coated with a single mesostructured film with a regularly arranged porosity.[17] In that case, a weak resonant mode is created in the outer layer. As we have recently shown, this resonance is very sensitive to variations of the refractive index of the porous coating, which facilitates the detection of any modification of the environment that may give rise to such a change. Due to the simple architecture of the ensemble, the relationship between reflectance measurements and the physicochemical modifications of the outer layer is readily made.

N. Hidalgo, Dr. M. E. Calvo, Dr. H. Míguez
Instituto de Ciencia de Materiales de Sevilla
Consejo Superior de Investigaciones Científicas-Universidad de Sevilla
Américo Vespucio 49, 41092 Sevilla, Spain
E-mail: hernan@icmse.csic.es
Dr. M. G. Bellino, Prof. G. J. A. A. Soler-Illia
Gerencia Química–Centro Atómico Constituyentes
Comisión Nacional de Energía Atómica
Av. Gral Paz 1499 (B1650KNA) San Martín
Buenos Aires, Argentina

DOI: 10.1002/adfm.201002486

To date, no resonator has been reported in which the presence of porosity is spatially restricted to the limits of the optical cavity. Such a structure, in which a porous slab would be surrounded by dense multilayers, should present a sharp and intense spectral optical resonance. Its response to external changes should also be easier to interpret, since modifications of the photon resonances would only be related to changes of the optical constants of the cavity due to the presence of adsorbed species, and not of those of the surrounding dense 1DPCs. Nevertheless, the feasibility of this proposal depends strongly on the ability to create a pore network that can be accessed from the external environment through its lateral outer surfaces.

In this work, a combination of sol-gel synthetic methods and coating techniques is employed to attain a dense multilayer structure in which the periodicity of the refractive index is disrupted by the presence of a middle porous mesostructured thin film. Such materials display clear dips in the reflectance spectrum associated with photon resonant modes localized in the porous midlayer, whose frequency varies as a response to the presence of specific compounds in the surrounding environment. We prove that the porous network of this optical cavity can be tailored to allow the entrance of small molecules while preventing the access of larger ones, hence showing the capability to selectively incorporate and thus detect species, depending on their size. As far as we know, this is the first optical resonator in which only the defect layer is porous, which greatly simplifies the analysis of the optical changes caused by variations in the environment. The resonator shows a sensitivity of a few nanomoles of solvent per cubic centimeter and an improved resolution over other environmentally responsive photonic structures containing mesostructured layers.

2. Results and Discussion

2.1. Structural and Optical Analysis of Porous Mesostructured Optical Resonators

The structure herein presented is a multilayer made of alternate dense SiO_2 and TiO_2 slabs, each one between 40–120 nm thick, which includes a thin TiO_2 porous mesostructured film (thickness between 50–300 nm) that breaks the spatial periodicity of the refractive index along the perpendicular direction and thus acts as an optical dopant. Such a middle layer presents a structure of interconnected pores of regular size with a range of between a few and tens of nanometers. The dense periodic multilayer was obtained by sequential dip-coating of SiO_2 and TiO_2 sol-gel precursors, which has been demonstrated to yield high-quality optical coatings.[18,19] The intermediate mesoporous slabs were deposited by dip-coating a supramolecularly templated partially hydrolyzed titanium oxide precursor.[20,21] We chose Pluronics F127 as the surfactant to attain the lyotropic mesophase that will yield an ordered void network after removal of the template. When films of very different thermal and mechanical properties are deposited onto one another, special care must be taken to prevent the collapse of the mesostructure, as well as cracking and delamination due to tensile stress induced by drying and heating. In the case of organically templated oxides these issues are particularly important. Full details of the synthesis and stabilization of the structure are given in the Experimental Section. In **Figure 1** we show field emission scanning electron microscopy (FESEM) images of a cross-section of a three-unit-cell periodic dense SiO_2–TiO_2 multilayer made with a TiO_2 mesoporous film embedded within. Layers of dense TiO_2 and SiO_2 are clearly identified as bright and dark stripes in Figure 1a, as a consequence of their different electronic density. Silica layers are amorphous, while TiO_2 layers present an anatase crystalline structure, as confirmed by X-ray diffraction (XRD), with an average crystal size of several tens of nanometers. The latter results from the large volume changes that take place during the thermal stabilization of the multilayer, which induces the crystallization of the originally amorphous TiO_2 layer. The thicker midlayer in Figure 1a is made of mesostructured titania and it can be seen that it does not alter the long-range uniformity of the total ensemble. The narrow pore-size distribution of the sandwiched periodic mesostructure is evident in Figure 1b. The thickness of the midlayer deposited onto the first multilayer may be precisely tuned through the concentration of the precursor and the withdrawal speed of the substrate in the range comprised between 50–300 nm, as has been demonstrated before.[17] This result stems from the fine control of mesostructured film thickness achievable by the combination of sol-gel methods and spin- or dip-coating techniques.[21]

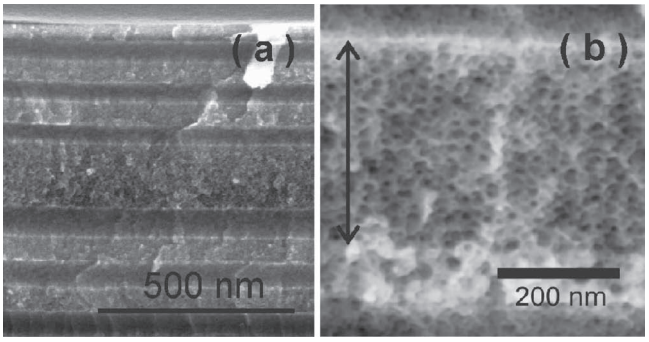

Figure 1. FESEM images of cross-sections of dense SiO_2–TiO_2 multilayers containing a porous mesostructured TiO_2 middle layer taken at a) low and b) high magnification.

An analysis of the pore and neck size of each type of porous layer employed to build the optical cavities was performed by means of poro-ellipsometry (data not shown). From this analysis, we could confirm that, as expected, the mesostructured film presents pores of 10-nm average diameter connected through 8-nm average diameter interpore necks. The control over the average pore size and the interpore windows permitted by this type of mesostructure is key to achieving the efficient infiltration of species, as will be shown in the next section. A similar investigation was carried out for the individual nontemplated layers, which were hence expected to be dense, to find out that 2% and 4% porosity (with a broad pore-size distribution, below 3-nm diameter) was present in the SiO_2 and TiO_2 films, respectively. As has been shown,[17] a small micropore volume does not affect the environmental optical response of the final structure although, as will be demonstrated later, this depends

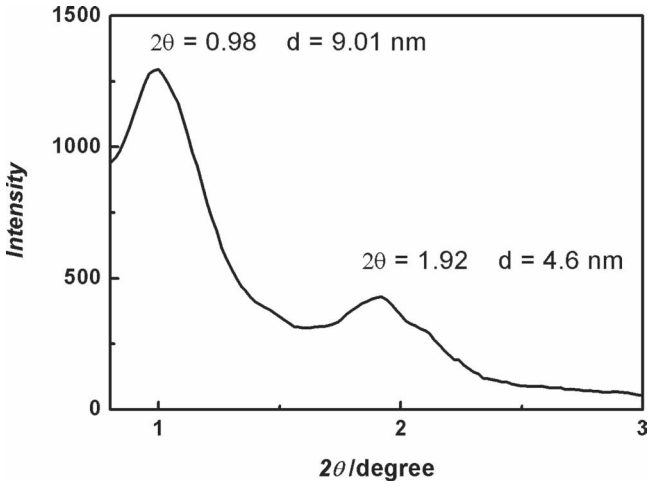

Figure 2. X-ray diffractogram of a dense periodic multilayer sandwiching a TiO_2 mesostructured film made using F127 as a template. Measurements were performed after elimination of the organic phase.

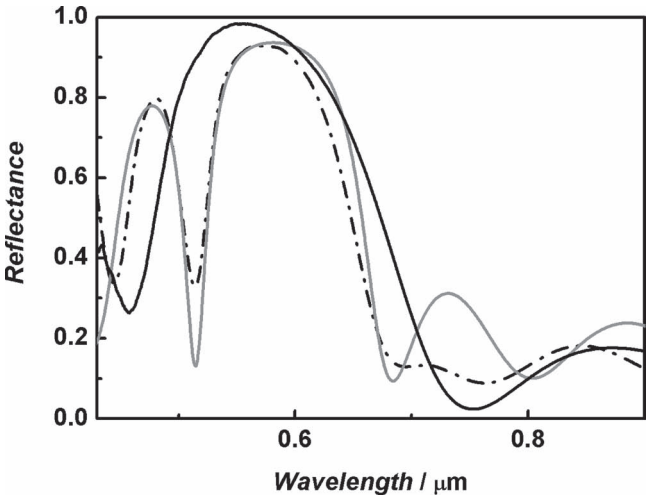

Figure 3. Specular reflectance spectra of a multilayer made of three unit cells consisting of alternate layers of dense TiO_2 and SiO_2 (black solid line) and the same structure containing a middle layer of mesostructured TiO_2 (black dash-dotted line). The fitting performed to estimate the structural and optical parameters is also plotted (gray solid line).

on the size of the probe. X-ray diffractograms were measured for the hybrid (porous–dense) multilayers. The sandwiched mesostructured film shows the presence of a well-defined peak detected at low X-ray scattering angles, as shown in **Figure 2**, which indicates that the film presents a uniaxially contracted cubic array, of crystallographic type *Im3m*, as was originally expected due to the concentration of compounds used to prepare the sol–gel precursor.[22] From both the FESEM images of the multilayer and XRD analysis, we estimate that the pores are oblate ellipsoids with an average major diameter in the range 8–10 nm with 4-nm thick walls, in good agreement with the values obtained from the porosimetry analysis of the individual layers prepared using F127 molecules as the templating mesophase. This result proves that the ordered mesostructure of the midlayer is preserved after all the stabilization treatments to which the multilayer is subjected. This fact is relevant since good connectivity and accessibility of the pore network in the sandwiched layer are crucial to achieve our goals.

It is well known that periodic multilayers behave like a 1DPC or Bragg reflector as a result of the modulation of the refractive index in the direction perpendicular to the substrate. Interference between the beams reflected and transmitted at each interface present in the multilayer impedes the propagation of a certain photon frequency range, and this can be easily identified in a reflectance spectrum as a primary maximum. The position of this Bragg peak depends on the layer's refractive index and thickness, the latter being controlled by the deposition conditions, which in our case are the concentration of the precursor and the withdrawal speed of the substrate. If the periodicity is disrupted by the presence of a middle layer of different optical thickness, which is defined as the product between its refractive index and its thickness, resonant modes localized within that intermediate slab are created. The fingerprint of such modes, and thus of an optical resonator, on the reflectance (transmittance) spectra is the opening of a transmission (reflection) window within the range of frequencies at which the Bragg peak arise. In **Figure 3** we plot the specular reflectance spectra attained from a three-unit-cell dense SiO_2-TiO_2 1DPC (black solid line) and from a multilayer in which an optical cavity has been built by embedding an ordered porous mesostructured TiO_2 film (black dash-dotted line). The fitting of the latter is also shown (gray solid line). For the case of purely dense 1DPCs, the high dielectric constant contrast between the alternating dense layers yields an intense and spectrally wide maximum. Secondary lobes are Fabry–Pérot oscillations resulting from the finite size of the structure. From the optimized fitting of these reflectance spectra using a MATLAB code based on the transfer-matrix approach,[23,24] we extract the refractive index n and the thickness of the different component layers. In the sample used for the detailed optical measurements, the unit cell of the dense Bragg mirror consists of a 80 ± 8-nm thick SiO_2 layer and a 65 ± 6-nm thick TiO_2 layer. The refractive indexes of these layers are 1.46 and 2.12, respectively. The mesostructured optical cavity has a thickness of 129 ± 13 nm and a refractive index $n = 1.80$.

2.2. Environmental Response of Porous Mesostructured Optical Resonators

In the previous section, we showed that, for those samples in which the periodicity is broken by the presence of the embedded mesostructured film, the effect of the resonant modes can be clearly identified in the reflectance spectra as dips spectrally located within the forbidden photonic band of the 1DPC. The spectral position of this reflectance dip associated with this resonant effect is strongly affected by changes in the refractive index of the porous mesostructured optical cavity. This sensitivity can be used to detect the presence of species adsorbed on the pore walls. In addition to what occurred for mesostructured coatings onto dense 1DPCs,[17] for which accessibility was mainly determined by the relation between channel and probe molecule sizes, for embedded resonators like the ones herein presented such capability will also depend on the ability

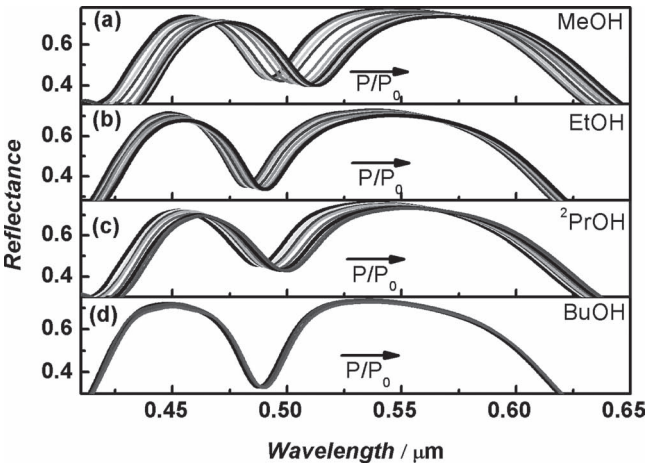

Figure 4. Series of reflectance spectra attained at different partial pressures of a) methanol, b) ethanol, c) 2-propanol, and d) butanol from mesostructured optical resonators with pores of average size 9 nm. The direction of increasing pressure is highlighted by an arrow.

of the probe molecules to penetrate the porous network of the embedded film from the sides, since the top and bottom surfaces of the cavity are surrounded by dense mirrors. To analyze the response of the network to changes in the environment, an optical resonator with high pore regularity is preferred, since it is the only one that can show size-selective effects. Such a resonator was exposed to increasing pressures (P) of a series of alcohols of different molecular size, namely, methanol, ethanol, 2-propanol, and butanol. A closed transparent chamber that was specifically designed for this purpose was used. Specular optical reflectance measurements were made in situ as pressure increased from $P/P_0 = 0$ up to $P/P_0 = 1$, where P_0 is the saturation pressure at room temperature. Results are shown in **Figure 4** for the whole series of solvents employed. The gradual shift observed is the direct consequence of the continuing increase of the refractive index of the pores when adsorption, and eventually condensation, of solvent molecules onto the mesopore walls takes place. This effect provides a precise means of detecting the presence of adsorbed species in the pores. The optimized fitting of all these spectra yields the estimated values of the effective refractive index for the, respectively, small and large pore mesostructured midlayer as P/P_0 increases.

By using the Bruggeman equation:

$$\frac{n_{TiO_2}^2 - n_{eff}^2}{n_{TiO_2}^2 + 2n_{eff}^2} ff_{TiO_2} + \frac{n_{void}^2 - n_{eff}^2}{n_{void}^2 + 2n_{eff}^2} ff_{void} + \frac{n_s^2 - n_{eff}^2}{n_s^2 + 2n_{eff}^2} ff_s = 0 \quad (1)$$

where n_{TiO_2}, n_{void} and n_s are the refractive indexes of the titanium oxide of the pore walls, the voids in the structure, and the solvent whose vapor pressure is gradually increased in the chamber, respectively, it is then possible to obtain information on the percentage of the original porosity filled by the solvent.[25] These data are plotted in **Figure 5**.

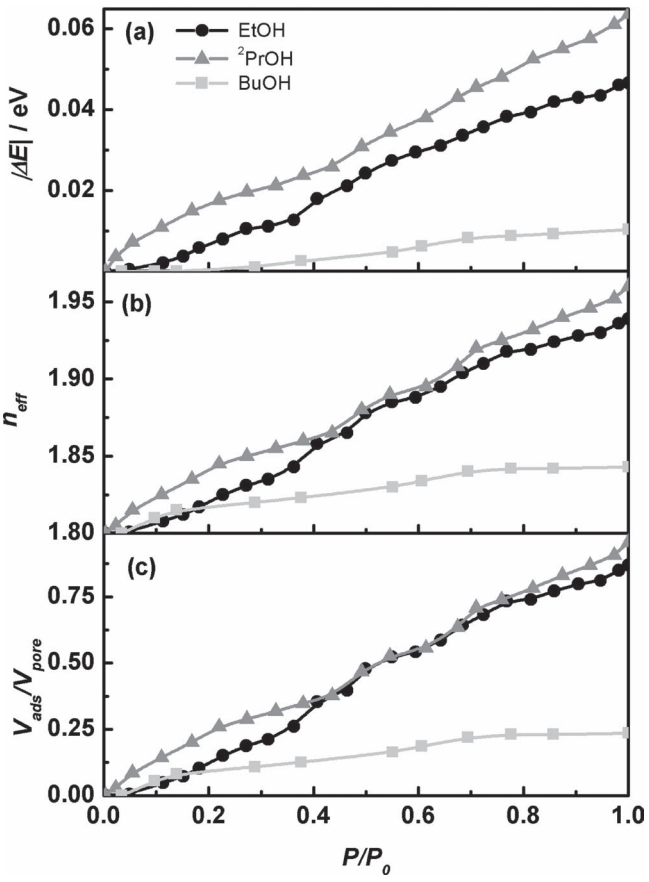

Figure 5. Variation of a) the spectral position of the optical resonance, b) the refractive index, and c) the percentage of filled porosity versus the partial pressure of the different solvents employed.

Several conclusions can be extracted after analyzing and comparing the different graphs displayed in Figures 4 and 5. Primarily, these results prove that the pore network is fully accessible for some of the probes tested even when it is surrounded by dense multilayers. Restrictions to the rate at which molecules enter the porous midlayer caused by its narrow lateral width are reflected in the times needed to reach equilibrium, which are longer than those observed for fully accessible mesoporous coatings.[16,26] In addition, the optical shifts caused by solvent adsorption are larger for smaller molecules, and are negligible for the largest probe tested (butanol), which highlights that accessibility strongly depends on the relationship between pore and analyte sizes. Interestingly, the detailed analysis of the reflectance spectra reveals that very small molecules like methanol are capable of diffusing through the small pores in the multilayers surrounding the mesostructured midlayer, which causes red-shifts of the resonant mode to occur even after 100% filling of the mesostructured film has been reached. For methanol, no results of the spectral analysis are depicted in Figure 5, since the complex interplay between the adsorption and condensation effects occurring for this small molecule in the different layers causes the analysis of the optical response to deviate from the simpler one expected for dense Bragg mirrors surrounding a mesoporous layer. On the other hand, larger probes (ethanol, 2-propanol) can only access the optical cavity, as

their effect on the resonant mode demonstrates. In these cases, the maximum filled porosity is 98% and 96% for ethanol and 2-propanol, respectively, and a larger spectral displacement is observed with the latter fluid due to its higher refractive index. In both adsorption isotherms obtained for ethanol and 2-propanol, for which full accessibility was confirmed, it should be noticed that there is no sign of sudden condensation as expected for a narrow pore-size distribution like the one herein attained and characterized by XRD, FESEM, and poro-ellipsosimmetry. Although a slight increase in the slope of the monotonically growing curves displayed in Figure 5c can be appreciated in the range $0.4 < P/P_0 < 0.45$, the trend is quasilinear up to the saturation pressure. This behavior indicates that there is a complex mechanism of capillary adsorption and transport through the confined layer that resembles that previously reported for other multilayered structures.[15]

2.3. Comparison Between the Environmental Response of Surface and Bulk Localized Resonant Modes

A comparison is presented in this section between the performance towards environmental changes of a mesostructured film placed either as an outer layer or as a defect buried within the 1DPC. When the former type of responsive multilayer was used to monitor changes of gas pressure in the surroundings,[17] equilibrium was reached faster, since outer porous layers can be accessed more rapidly than buried ones. However, the effect of the resonance on the optical response is much more pronounced in the latter, as can be readily seen in **Figure 6**a; greater confinement of the electromagnetic field

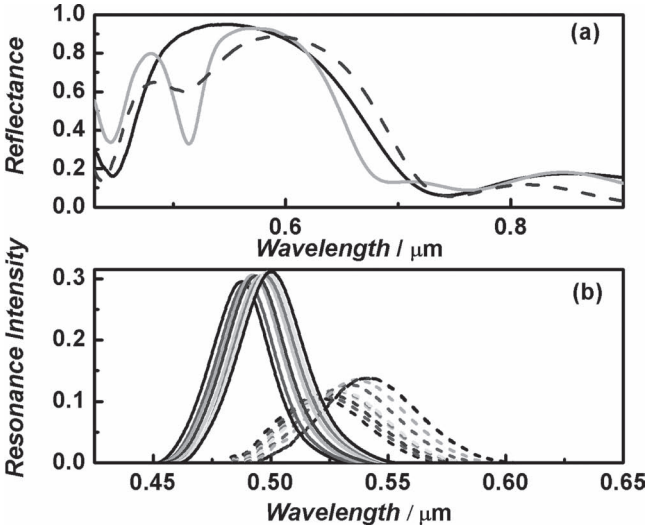

Figure 6. a) Specular reflectance spectra of a dense multilayer (black solid line), a similar multilayer coated by a porous mesostructured film of thickness 267 ± 20 nm (dark gray dashed line), and an optical resonator prepared by embedding a porous mesostructured layer of thickness 129 ± 13 nm between two periodic multilayers (light gray solid line). b) Variation of the resonant peaks measured as the partial pressure of 2-propanol increases in the chamber, extracted from the specular reflectance spectra, for a multilayer either with an embedded porous mesostructured layer (solid lines) or coated with one (dashed lines).

in the buried porous layer is accompanied by deeper and spectrally narrower reflection dips occurring at photonic band-gap frequencies, which results in a finer spectral resolution when detecting gas-pressure changes. To show this explicitly, we have prepared a 1DPC coated with a thick mesostructured film of a thickness of 198 ± 20 nm, whose optical response was optimized to show resonant bands in the reflectance spectrum as well-defined as possible, and a 129 ± 13 nm mesostructured defect layer that acts as an optical cavity when buried between two 1DPCs. Independent of its position in the multilayer, the refractive index of the mesostructured layer is $n = 1.80$. Please notice that one major advantage of these latter optical cavities is that pronounced reflectance dips are attained for embedded layers of almost any available thickness, while for the case of outer layers, only very thick ones yield intense effects on the spectra.[17] In Figure 6b we plot the series of resonant bands measured from 1DPC structures containing either outer or inner mesoporous layers as the partial pressure of 2-propanol increases in the chamber. For the sake of clarity, results for samples displaying resonant bands at different spectral regions are shown. Dips have been extracted from the corresponding reflectance spectra by substracting the nonlinear background and converted into positive intensity peaks to allow easy comparison between them. From these plots we can readily estimate the quality factor (Q) of the resonance in each case, defined as the ratio between the central position of the resonant peak and its full width at half maximum. This estimation yields average values around $Q \approx 10$ and $Q \approx 20$ for the 1DPCs containing either optimized outer or standard inner porous layers, respectively. To estimate the effect of this different value of Q on the resolution achieved when using either type of material for detecting gas-pressure changes, we calculate the ratio between the area $\int_i$ of a resonant peak measured at a certain pressure P_i and that of the region of overlap $\int_{ov}$ between that initial peak and another one measured at a higher pressure P_f. This calculation was done for a wide range of pressures and the results were normalized by the partial pressure increment $(P_f - P_i)/P_0$ in each case. The higher this number, i.e., the lower the overlap between adjacent peaks, the better the resolution achieved. Results for both types of multilayers are displayed in **Figure 7**. It can be readily seen that the buried mesostructured film (black circles and solid connecting line) provides higher resolution than the outer one (gray circles and dashed connecting line) for most of the pressure ranges analyzed; this is one of the main advantages of the new resonant structure herein presented. Regarding the sensitivity, the modification of the resonant peaks measured at the lower pressure range allows us to detect mass variations of a few nanomoles per cubic centimeter in both cases.

3. Conclusion

Our results demonstrate a synthetic route to attain high-optical-quality dense periodic multilayered structures in which the translational symmetry is broken by the presence of a middle mesostructured thin film of high and accessible porosity. The sensitivity of the spectral position of the photon resonance to environmental changes is confirmed by performing isothermal optical reflectance measurements under controlled

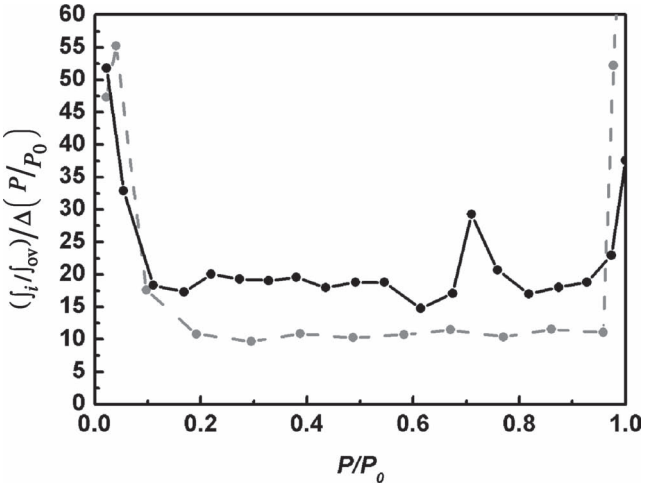

Figure 7. Comparative plot showing the experimentally estimated resolution achieved when detecting gas-pressure changes using a 1DPC coated with (gray circles and dashed line) or with an embedded (black circles and solid line) porous mesostructured layer.

vapor-pressure conditions. The importance of the interplay between pore and probe-molecule diameters is studied and its implications in size-selective detection discussed. Results are compared to those attained for other types of mesostructured films coupled to photonic crystals as outer layers, with a higher resolution being found for porous films embedded in a photonic crystal due to the narrower and more intense resonant peak detected. The optical performance of supramolecularly templated mesoporous optical resonators built in one-dimensional photonic crystals may be put into practice in the development of new sensing devices, which are sensitive to the environment yet robust.

4. Experimental Section

Preparation of the Porous Mesostructured Optical Resonators: Optical porous resonators were prepared in three stages. First, a dense 1D photonic crystal was built by the alternate dip-coating deposition of TiO_2 and SiO_2 sols. Next, the mesoporous layers were incorporated into this structure by dip-coating the precursor sol, and finally another dense 1D photonic crystal was deposited on top of the porous layer.

Synthesis and Deposition of Dense TiO_2 and SiO_2 Layers: TiO_2 and SiO_2 sols were prepared following procedures described elsewhere.[18,19] The substrates used were standard microscope glass slides and they were cleaned with an HNO_3 solution (5%), water and, finally, with ethanol. The SiO_2 sol was synthesized using tetraethylorthosilicate (4.5 mL, TEOS, Merck) and absolute ethanol (34 mL, EtOH). After some minutes under vigorous stirring, H_2O (1.72 mL) and HCl 0.05 N (0.08 mL) were added. To prepare the TiO_2 sol, titanium isopropoxide (2.5 mL, TIPT, 97%, Aldrich), HNO_3 1M (0.156 mL), H_2O (0.078 mL), and 2-propanol (25 mL, ^{2}PrOH, Aldrich) were mixed and stirred. The multilayer was prepared by dip-coating both sols alternately by employing a dip-coater (HWTL-01-A, MTI Corporation). In each case the substrate was immersed into the sol and lifted at a controlled speed. The speed was varied between 0.5 and 2 mm s^{-1}, which allowed us to attain thicknesses in the 50–200 nm range. Each layer was heated at 300 °C for 1 h to stabilize it before depositing a new one.

Synthesis and Deposition of Mesoporous Layers: A sol was prepared by adding an organic template $(EO)_{106}(PO)_{70}(EO)_{106}$ (commercial name Pluronics F127, Aldrich Inc.) where EO stands for ethylene oxide and PO for propylene oxide monomers, to a $TiCl_4$:EtOH 1:40 solution (20 mL). In this case the polymer (0.573 g) and water (1.61 mL) were mixed over 30 min into the alcoholic solution and then kept at 4 °C.

To coat the first dense multilayer with this precursor sol, we also used a dip-coating process. After the deposition, the samples were introduced into a 50% relative humidity chamber for 24 h, then thermally stabilized it at 60 °C and 120 °C over 24 h and finally at 200 °C for 2 h. In some cases we needed to make a second deposition of the sol to obtain a mesoporous layer with greater thickness.

After the thermal stabilization of the mesoporous structure, we deposited the second dense photonic crystal onto the structure using the same methodology as for the initial 1D photonic crystal. To stabilize the overall structure and to remove the organic template we used a thermal treatment at 350 °C for 1 h (ramp 1 °C min^{-1}).

Structural Characterization: Pore and neck size were characterized in films deposited individually onto glass substrates through environmental ellipsometric porosimetry. Water adsorption–desorption isotherms were determined at 298 K by environmental ellipsometric porosimetry (EEP) using a SOPRA GES5A apparatus, equipped with microspot optics. Film thickness and the real component of the refractive index were obtained by fitting the ellipsometric parameters $\psi(\lambda)$ and $\Delta(\lambda)$ in the 400–800 nm spectral range; the film refractive index was described according to a modified Cauchy equation. The WinElli 2 software (Sopra Inc), which transforms the variation of n with P/P_0 into filled pore volume by using a three-medium BEMA treatment, was used. Pore- and neck-size distributions were derived according to a Kelvin model.[22] X-ray diffractograms of the films were attained using a Siemens D501 apparatus operating with an averaged wavelength λ_{Cu} = 1.54 Å in θ-2θ geometry. Electron microscopy images were obtained using a field emission microscope Hitachi 5200 operating at 2kV.

Analysis of the Optical Properties and their Environmental Dependence: Optical characterization of the porous resonators was performed using a Fourier-transform infrared spectrophotometer (BRUKER IFS-66) attached to a microscope and operating in reflection mode. An X4 objective with a numerical aperture of 0.1 (light cone angle ±5.7°) was used to irradiate the samples and collect the reflected light at quasinormal incidence with respect to their surface. A spatial filter was used to selectively detect light from 1 mm^2 circular regions of the sample. Optical response to environmental changes was measured using a closed transparent chamber, specifically designed for this purpose. Specular optical reflectance measurements were recorded in situ as pressure increased from P/P_0 = 0 up to P/P_0 = 1. Vapor pressure in the chamber was regulated by the controlled and gradual release of a fixed amount of solvent vapor. Each measurement was made after equilibrium has been reached, which typically occurred after 5 min.

Acknowledgements

We thank the Spanish Ministry of Science and Innovation for funding provided under grants MAT2008–02166 and CONSOLIDER HOPE CSD2007–00007, to Junta de Andalucía for grant FQM3579, and to ANPCyT (PICT-34518, PICT-00335, and PAE-37063/PME-00038). M.E.C. thanks the Junta de Andalucía and the Spanish Research Council for funding of his contract under the JAE program. M.G.B. and G.J.A.A.S-I. are members of CONICET; M.E.C and G.J.A.A.S.I. are members of Gabbo's.

Received: November 24, 2010
Published online: May 5, 2011

[1] K. A. Kilian, T. Böecking, J. J. Gooding, *Chem. Commun.* **2009**, *6*, 630.
[2] S. Colodrero, M. Ocaña, A. R. González-Elipe, H. Míguez, *Langmuir* **2008**, *24*, 9135.

[3] S. Y. Choi, M. Mamak, G. von Freymann, N. Chopra, G. A. Ozin, *Nano Lett.* **2006**, *6*, 2456.
[4] B. V. Lotsch, G. A. Ozin, *Adv. Mater.* **2008**, *20*, 4079.
[5] O. Sánchez-Sobrado, M. E. Calvo, N. Núñez, M. Ocaña, G. Lozano, H. Míguez, *Nanoscale* **2010**, *2*, 936.
[6] S. Colodrero, A. Mihi, L. Häggman, M. Ocaña, G. Boschloo, A. Hagfeldt, H. Míguez, *Adv. Mater.* **2009**, *21*, 764.
[7] F. Scotognella, D. P. Puzzo, A. Monguzzi, D. S. Wiersma, D. Maschke, R. Tubino, G. A. Ozin, *Small* **2009**, *5*, 2048.
[8] A. M. Vredenberg, N. E. J. Hunt, E. F. Schubert, D. C. Jacobson, J. M. Poate, G. J. Zydzik, *Phys. Rev. Lett.* **1993**, *71*, 517.
[9] V. S. Y. Lin, K. Motesharei, K. P. S. Dancil, M. J. Sailor, M. R. Ghadiri, *Science* **1997**, *278*, 840.
[10] J. J. Steele, A. C. van Popta, M. M. Hawkeye, J. C. Sit, M. J. Brett, *Sens. Actuators B* **2006**, *120*, 213.
[11] S. Colodrero, M. Ocaña, H. Míguez, ES2304104 (WO2008102046), **2007**.
[12] S. Colodrero, M. Ocaña, H. Míguez, *Langmuir* **2008**, *24*, 4430.
[13] M. C. Fuertes, G. J. A. A. Soler-Illia, H. Míguez, EP2073045 (WO2008034932), **2006**.
[14] M. C. Fuertes, F. J. López-Alcaraz, M. C. Marchi, H. E. Troiani, V. Luca, H. Míguez, G. J. de A. A. Soler-Illia, *Adv. Funct. Mater.* **2007**, *17*, 1247.
[15] M. C. Fuertes, S. Colodrero, G. Lozano, A. R. González-Elipe, D. Grosso, C. Boissiere, C. Sanchez, G. J. A. A. Soler-Illia, H. Miguez, *J. Phys. Chem. C* **2008**, *112*, 3157.
[16] J. Kobler, B. V. Lotsch, G. A. Ozin, T. Bein, *ACS Nano* **2009**, *3*, 1669.
[17] N. Hidalgo, M. E. Calvo, H. Míguez, *Small* **2009**, *5*, 2309.
[18] B. E. Yoldas, *J. Mater. Sci.* **1986**, *21*, 1087.
[19] K. A. Cerqua, J. E. Hayden, W. C. LaCourse. *J. Non-Cryst. Solids* **1988**, *100*, 471.
[20] G. J. A. A. Soler-Illia, P. Innocenzi, *Chem. Eur. J.* **2006**, *12*, 4478.
[21] C. Sanchez, C. Boissière, D. Grosso, C. Laberty, L. Nicole, *Chem. Mater.* **2008**, *20*, 682.
[22] E. L. Crepaldi, G. J. A. A. Soler-Illia, D. Grosso, F. Cagnol, F. Ribot, C. Sanchez, *J. Am. Chem. Soc.* **2003**, *125*, 9770.
[23] J. M. Bendickson, J. P. Dowling, M. Scalora, *Phys. Rev. E* **1996**, *53*, 4107.
[24] G. Lozano, S. Colodrero, O. Caulier, M. E. Calvo, H. Míguez, *J. Phys. Chem. C* **2010**, *114*, 3681.
[25] D. A. G. Bruggeman, *Ann. Phys.* **1935**, *24*, 636.
[26] V. Rouessac, R. Coustel, F. Bosc, J. Durand, A. Ayral, *Thin Solid Films* **2006**, *495*, 232.